Transparent Mineral Sunscreen with Non-Nano Rod-Shaped Zinc Oxide

Kyounghee Shin, Sungsuk Byeon, Yeonggi Kim, **Sungho Lee***

R&D Center, SUNJIN BEAUTY SCIENCE Co., Ltd., Republic of Korea

*Dr. Sungho Lee
Address: Gasan Digital 2-ro, Seoul, Republic of Korea
TEL: +82-2-853-3200
Email address: sungholee@sunjinbs.com

Abstract (Maximum of 200 words)
Driven by the increasing global focus on sunscreen efficacy and safety, researchers are actively developing novel inorganic ultraviolet (UV) filters. Stringent EU regulations on nanomaterials have spurred a gradual shift away from nano-sized sunscreens. Additionally, the growing concern about potential skin penetration of chemical UV filters has fueled the development of mineral-only sunscreen formulations. In response to these trends, this study investigated the potential of non-nano, rod-shaped zinc oxide (ZnO) for improved mineral-only sunscreens. Synthesized rod-shaped ZnO particles exhibited good control over size and aspect ratio. These particles were successfully dispersed in oil using various surface modification techniques. The rod-shaped ZnO displayed improved transparency and texture compared to conventional spherical ZnO particles. Importantly, in vivo studies confirmed that this translated to enhanced UV protection, even surpassing formulations containing regular non-nano ZnO. These findings suggest that rod-shaped ZnO offers a promising approach for developing safer and more cosmetically pleasing sunscreens.

Keywords: Non-nano, Zinc oxide, Rod-shape, UV Protection, Sensory feel, Transparency

Introduction.

Mineral sunscreens are gaining popularity due to growing concerns about the safety of organic UV filters and their negative impact on the environment, particularly coral reefs and marine ecosystems. These mineral sunscreens, using inorganic UV filters like zinc oxide and titanium dioxide, offer immediate broad-spectrum protection without harming the environment [1-2]. This makes them a safer and more sustainable choice for sun protection. Despite these advantages, mineral sunscreens face challenges in user experience. Compared to organic UV filters, they can be less spreadable and leave a noticeable white cast, particularly on darker skin tones [3]. To minimize these limitations, researchers have primarily focused on incorporating nano-sized mineral filters (inorganic UV filters less than 100 nm in size) into mineral sunscreens. While this approach improves spreadability and reduces white cast, it has raised concerns about potential human health risks associated with nanoparticles [4-5]. This highlights the need for a novel mineral sunscreen that strikes a balance between safety, efficacy, and consumer experience.

Among the diverse nanoparticle shapes, spherical and rod nanoparticles stand out as prominent choices for sun protection formulations [6-9]. However, their distinct physical characteristics lead to significant differences in agglomeration, self-assembly, and friction-induced skin feel, influencing their overall performance and consumer experience. Spherical nanoparticles exhibit a strong tendency to form tightly packed, three-dimensional aggregates due to their high surface-to-volume ratio and isotropic nature [10-11]. These aggregates can

lead to increased particle size, potentially affecting formulation stability and UV protection efficacy. The formation of agglomerates can also impact the sunscreen's physical appearance, potentially resulting in a grainy or chalky texture. Rod nanoparticles display a lower propensity for agglomeration compared to spherical nanoparticles due to their anisotropic shape and reduced surface-to-volume ratio [12]. This reduced agglomeration tendency can lead to more uniform particle dispersion, potentially enhancing dispersion stability, transparency, and UV protection efficacy. Moreover, the lack of agglomeration can also contribute to a smoother sunscreen texture. These advantages of rod-shaped particles suggest the possibility of using them even in non-nano sizes while maintaining these desirable qualities.

The demand for sunscreens that are both effective and cosmetically appealing continues to propel advancements in sun protection technology. This study investigates the potential of non-nano, rod-shaped inorganic UV filters, specifically zinc oxide (ZnO), for improved sunscreen formulations. Their unique shape offers advantages in terms of dispersion, transparency, and potentially reduced health risks compared to conventional nanoparticles. By successfully synthesizing and characterizing these rod-shaped ZnO particles, we aim to contribute to the development of safer and more cosmetically pleasing sunscreens.

Materials and Methods.

1. Synthesis of rod-shaped zinc oxide

Hydrothermal method was used to obtain non-nano, rod-shaped ZnO. $ZnCl_2$ was first dissolved in distilled water. To achieve the desired non-nano, rod-shaped ZnO (ZnO 200), alkali solution was slowly added to the precursor solution under mild stirring, with the pH carefully monitored and maintained at 7 through neutralization. Then, the hydrophobic coating agent was added into the solution. After that, it was kept in an oven at 140 °C until it got dried. Finally, the sample was pulverized with a jet mill.

Table 1. Synthesized ZnO particle and their information

Abbreviation	Composition	ZnO (purity)*	Size (nm)**	Shape**
ZnO 200AS	Zinc oxide, Triethoxycaprylylsilane	95%	200 nm × 60 nm	Rod
ZnO 200SA	Zinc oxide, Stearic acid	95%	200 nm × 60 nm	Rod
ZnO 200CA	Zinc oxide, Cetyl alcohol	95%	200 nm × 60 nm	Rod
ZnO NAS	Zinc oxide, Triethoxycaprylylsilane	97%	40 ± 10 nm	Round
ZnO AS	Zinc oxide, Triethoxycaprylylsilane	97%	150 ± 15 nm	Round

*Measured by ICP (inductively coupled plasma spectrometer)
**Tested by SEM

2. Characterization of rod-shaped zinc oxide

To confirm the acquisition of a crystalline phase attributed to the ZnO 200, an X-ray diffraction (XRD) analysis of the samples was performed. XRD patterns were made at room temperature with a step size of 0.05° in the angular range of 20–80° in 2θ, using a D8 Advance

Diffractometer (Bruker, Germany) with the copper $K_{\alpha 1}$ radiation (λ = 1.5406 Å). The surface morphology of the ZnO 200 was analyzed using scanning electron microscopy (SEM) (Zwess, Germany). The ZnO 200 treated with coating agents was further analyzed to identify organic residue and surface functional groups. Their infrared spectra were recorded using Fourier-transform infrared spectroscopy (FT-IR).

The transparency and texture of the ZnO samples were evaluated by visually assessing samples applied to the skin. For this evaluation, 1g of ZnO powder was applied to a designated area of the skin. In addition, the white index of ZnO dispersions was measured using a Chroma meter (Konica Minolta, Japan) and Draw down bar film applicator. These dispersions were prepared by mixing 30% ZnO powder with 70% cyclopentasiloxane.

The coating strength of the hydrophobically coated ZnO was tested by boiling an aqueous solution of ZnO powder at 100°C for 10 minutes. This aqueous solution was prepared by mixing 4 g of ZnO powder with 100 g of water.

3. Sunscreen formulation

The sunscreen formulation was developed using hydrophobically coated ZnO powder (ZnO 200AS), and then their UV protection performance was evaluated by *in vitro* and *in vivo* SPF and PA test. Solar light SPF-290AS (Solar light, USA) was used for *in vitro* SPF and PA measurements. A specimen with a thickness of 0.75 mg/cm^2 was applied on a poly methyl methacrylate (PMMA; USA) plate and dried for 15 min. After 4 MED pre-light irradiation, the UV protection index was measured using SPF-290AS. The average values of the measured readings at nine different positions of the PMMA plate were considered the final SPF and PA. *In vivo* SPF & PA measurement was performed by clinical experiments in accordance with the ISO-244444 International Cosmetics Autonomous Convention Act. PA was measured according to ISO-24442.

Results and Discussion.

Figure 1 presents SEM micrographs of the synthesized rod-shaped ZnO particles. The SEM images clearly revealed the rod-shaped morphology of the ZnO particles. The approximate particle size for ZnO 200AS is estimated to be 200-300 nm in length and 30-80 nm in width. Interestingly, the aspect ratio of the particles was controlled by their neutralization speed during synthesis. Slower neutralization resulted in the formation of longer, rod-shaped ZnO.

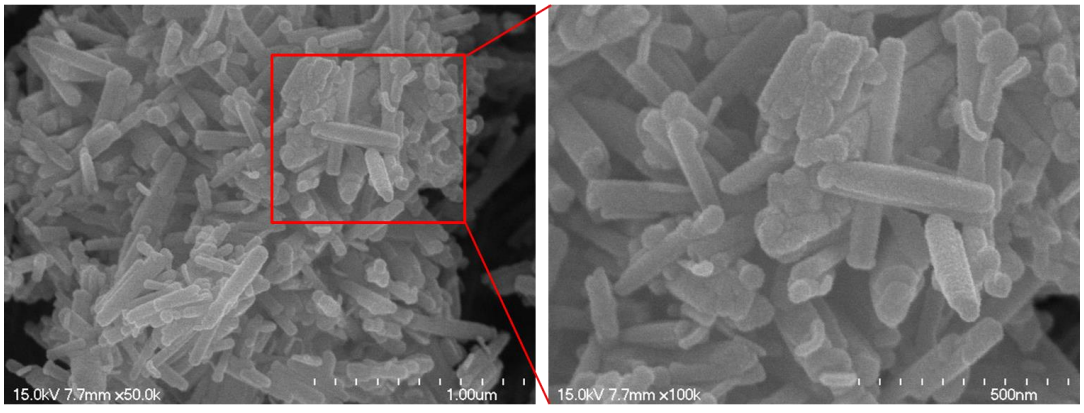

Figure 1. SEM images of synthesized ZnO 200AS.

The obtained XRD pattern indicates all the characteristic peaks observed in synthesized ZnO 200 are in a good agreement with the standard data of ZnO standard taken from the Joint Committee of Powder Diffraction Standard (JCPDS) card No. 36-1451 [13] and reference [14] (Figure 2). The XRD pattern also exhibits no significant diffraction peaks related to impurities, which confirms the high purity of the synthesized ZnO 200 obtained in this study.

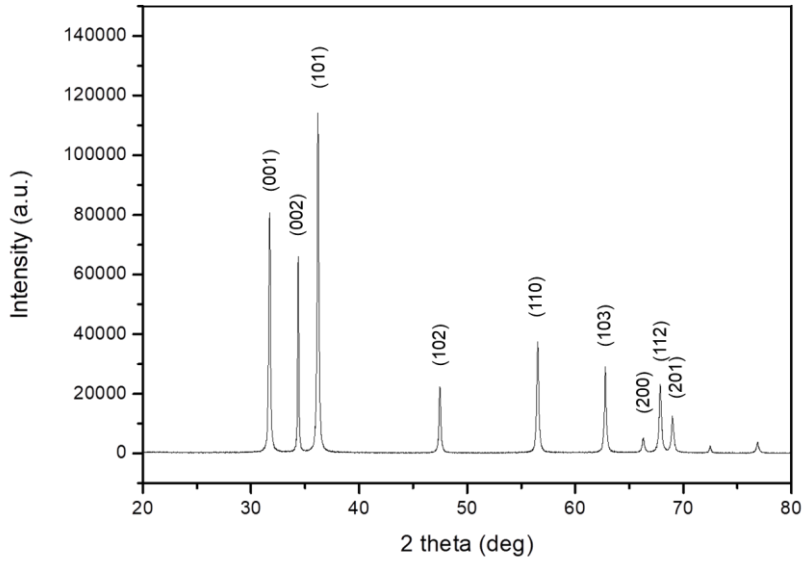

Figure 2. XRD pattern of synthesized ZnO 200.

Table 2. XRD analysis data of synthesized rod-shaped ZnO

Peak No	*hkl*	JCPDS No. 36-1451 2θ (deg)	Ref*. ZnO 2θ (deg)	ZnO 200 2θ (deg)	ZnO 200 Intensity (a.u.)
1	(100)	31.749	31.8	31.75	80,953
2	(002)	34.228	34.43	34.35	66,255
3	(101)	36.257	36.31	36.18	114,002
4	(102)	47.257	47.58	47.46	22,299
5	(110)	-	56.59	56.51	37,747
6	(103)	-	62.90	62.75	29,040
7	(200)	-	66.40	66.27	4,932
8	(112)	-	67.90	67.85	23,563
9	(201)	-	69.20	69.00	12,750

*Reference: [14]

Because of its relatively low reflective index, large-sized ZnO particles can be incorporated into formulations without causing significant whitening. This makes them ideal for formulating gentle, hypoallergenic sunscreens that offer UVA and UVB protection for babies and individuals with

sensitive skin. To improve dispersion within the formulas and enhance its performance as a UV filter, ZnO can be surface-treated with various organic compounds. In this study, surfaces of ZnO 200 were modified with hydrophobic materials such as triethoxycaprylylsilane, stearic acid, and cetyl alcohol. The modified ZnO particles were named ZnO 200AS, ZnO 200SA, and ZnO 200CA, respectively. The successful hydrophic modification was investigated by FT-IR analysis (Figure 3a). Figure 3b displays the UV/vis absorption spectra of both the synthesized ZnO 200 modified with various hydrophobic materials. Interestingly, the maximum absorption peak of the rod-shaped ZnO 200AS appeared around 330-360 nm, exhibiting a slight "blue shift" compared to typical nano-sized spherical ZnO AS (360-380 nm). This shorter wavelength peak can be attributed to the unique morphology of ZnO 200, characterized by smaller secondary particles [15-16]. Notably, other hydrophobically modified ZnO 200 particles displayed similar behavior. This unexpected result suggests that despite exceeding 100 nm in size, ZnO 200 offers UV protection comparable to nano-sized ZnO, making it a potentially valuable material for sunscreens.

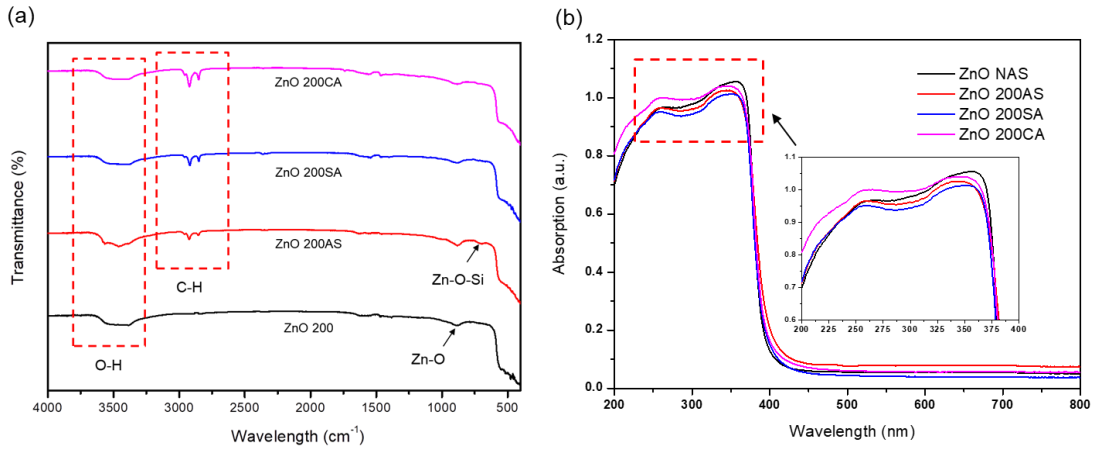

Figure 3. (a) FT-IR spectra of bare ZnO (ZnO 200) and hydrophobically modified rod-shaped ZnO particles and (b) UV/vis spectra of nono sized spherical shaped ZnO particle and non-nano rod-shaped ZnO particles.

The strength of the hydrophobic coating was evaluated by observing the hydrophobicity of the particles after boiling aqueous solutions of the modified ZnO (Figure 4). This assessment helps determine how well the hydrophobic material adheres to the ZnO surface. Interestingly, the coating stability of ZnO 200SA was similar to that of silane-coated ZnO particles (ZnO NAS, ZnO AS, and ZnO 200AS) formed by covalent bonds, even after boiling at 100°C. This suggests strong attachment of the coating to the ZnO surface. In contrast, ZnO 200CA migrated to the water phase after just 5 minutes of heating. This indicates detachment of the coating layer, exposing the bare ZnO. Consequently, ZnO 200AS and ZnO 200SA were chosen for further formulation.

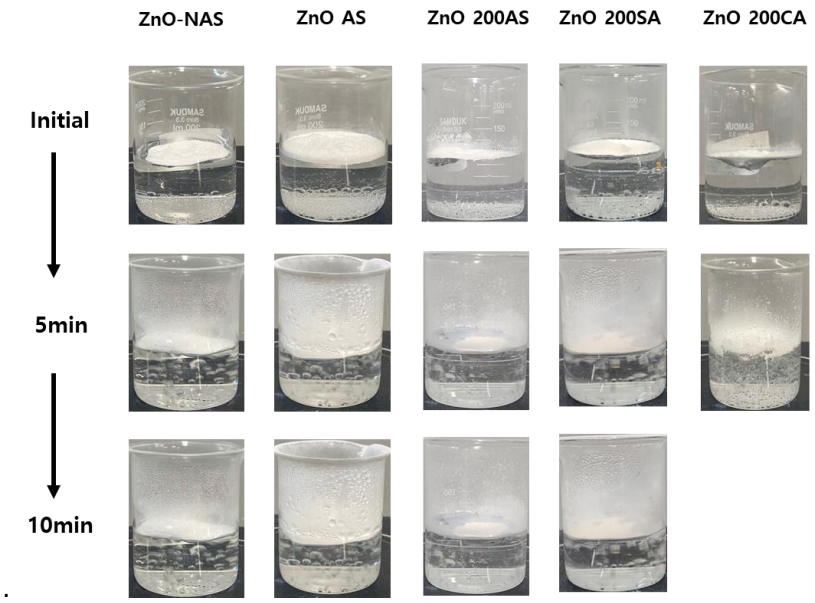

Figure 4. Coating stability test of hydrophobically modified ZnO particles.

To assess texture and transparency, the rod-shaped ZnO 200AS was compared to spherical ZnO particles of two sizes: 40 ± 10 nm (ZnO NAS) and 150 ± 15 nm (ZnO AS). As shown in Figure 5, the ZnO 200AS exhibited better spreadability and a softer texture than ZnO NAS, confirmed by their lower friction force. This is likely due to the reduced particle aggregation (smaller secondary particle) caused by the unique rod-shaped morphology. Additionally, the white index of ZnO oil dispersions was evaluated using a Draw Down method. Interestingly, ZnO 200AS exhibited higher transparency compared to ZnO AS, even though both are non-nano sized particles. These results suggest that the rod-shaped morphology improves the skin feel and transparency of ZnO for skin application.

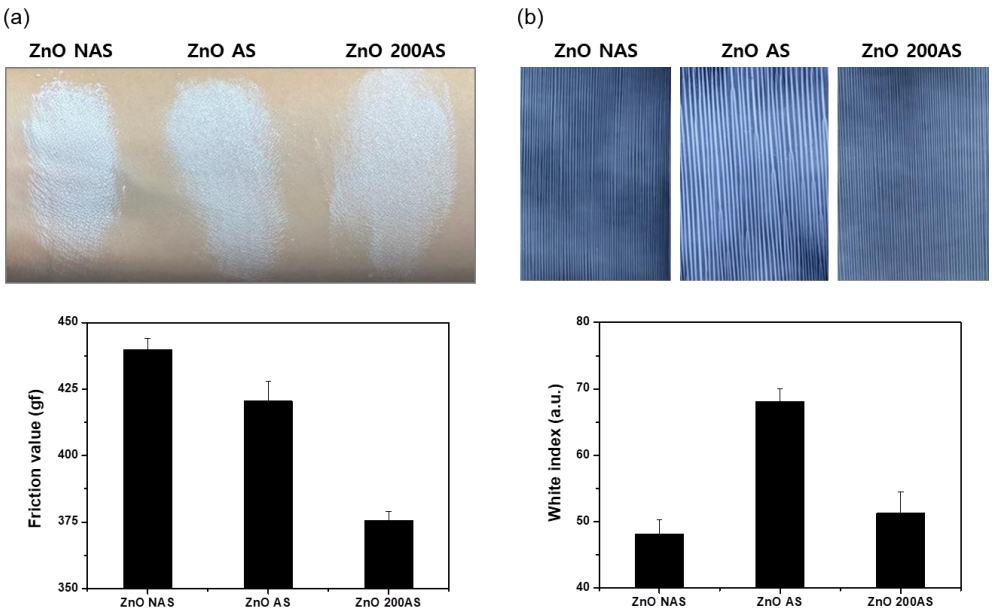

Figure 5. (a) Images of the ZnO powders applied to the skin and their friction value. (b) Images of the ZnO oil dispersion applied to the drawdown sheets and their white index. All the results were obtained from three replicate experiments.

Given the increased transparency and softer texture of the rod-shaped ZnO particles, we hypothesized that they would offer improved UV protection due to better spreadability on the skin. To confirm this, we conducted an *in vitro* SPF and PA test of W/O type suncare formulation using the ZnO powders (Table 3). Our tests showed that the ZnO 200AS significantly improved UV protection. It achieved an SPF of 23.8 and PA of 19.8, which is much higher than the values for ZnO AS (Figure 6). Importantly, these results were comparable to those of ZnO NAS, the powder with the strongest UV protection effect among all those tested. Clinical evaluation of the SPF index and PA grade according to size indicate the same tendency as that observed in vitro. When comparing the UV protection effect according to size and morphology, ZnO NAS, which exhibits nano-sized spherical shape, produces the highest UV protection index. We achieved the development of a sunscreen formulation containing only non-nano mineral filters. This formulation utilizes rod-shaped ZnO dispersions and delivers a high SPF of 50 and PA of 16. Notably, it outperforms formulations containing non-nano ZnO AS, despite having the same composition except for ZnO particles.

Table 3. Ingredients of the W/O suncare formulation

	Ingredient	Formula (w/w, %)		
		ZnO NAS	ZnO AS	ZnO 200AS
A	Coco-caprylate/caprate	11.0	11.0	11.0
	Carpylic/Capric Triglyceride	2.0	2.0	2.0
	Undecane & Tridecane	8.0	8.0	8.0
	Polyglyceryl-3 Polyricinoleate & Sorbitan Isostearate	5.0	5.0	5.0
	Coco-caprylate/caprate	2.0	2.0	2.0
B	Zinc oxide & Triethoxycaprylylsilane	25		
	Zinc oxide & Triethoxycaprylylsilane		25	
	Zinc oxide & Triethoxycaprylylsilane			25
C	Water	38.0	38.0	38.0
	Glycerin	5.0	5.0	5.0
	Sodium chloride	1.0	1.0	1.0

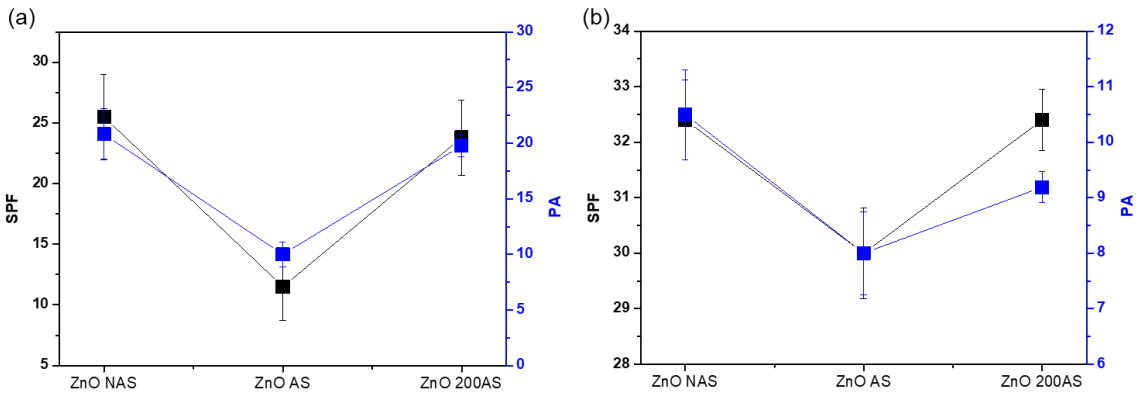

Figure 6. (a) *In vitro* SPF/PA and (b) *in vivo* PA of W/O suncare formulations containing hydrophobically modified ZnO particles. (n= 10).

Conclusion.

This study successfully synthesized rod-shaped ZnO particles and demonstrated their potential for improved sunscreens. The rod-shaped morphology offered several advantages, including dispersion stability, a softer texture on the skin, and higher transparency compared to conventional spherical ZnO particles. This resulted in a significant enhancement of UV protection efficacy (SPF and PA) in a sunscreen formulation containing only non-nano mineral filters. These findings suggest that rod-shaped ZnO is a promising candidate for developing safe and user-friendly sunscreens with high performance.

Acknowledgments.

This research was supported by a grant of the Korea Health Technology R&D Project through the Korea Health Industry Development Institute (KHIDI), funded by the Ministry of Health & Welfare, Republic of Korea (grant number: RS-2024-00340429).

Conflict of Interest Statement.

There are no conflicts to declare.

References.

1. Serpone N., Dondi D., Albini A (2007). Inorganic and organic UV filters: Their role and efficacy in sunscreens and suncare products. *Inorganica Chimica Acta,* 360(3), 794-802.
2. DiNardo J. C., Downs C. A. (2018). Dermatological and environmental toxicological impact of the sunscreen ingredient oxybenzone/benzophenone-3. *Journal of Cosmetic Dermatology,* 17(1),15–19.
3. Trees G. S., Stanislav P., (2011). Titanium dioxide and zinc oxide nanoparticles in sunscreens: focus on their safety and effectiveness, 25:95-112.
4. Chayada C., Thanisorn S., Titinun K., Monthatip B., Norramon C., Supisara W., Waranya B. (2021) Ultraviolet filters in sunscreens and cosmetic products - a market survey. *Contact Dermatitis*, 85(1), 58-68.
5. Ana J., Ines A., Joana D.,,Emilia S., Honorina C., Maria T. C., Jose M., Sousa L., Isabel F. (2022). Recent Trends on UV filters. *Applied Sciences*, 12(23), 12003.

6. Bin L., Hua C. Z. (2004). Room Temperature Solution Synthesis of Monodispersed Single-Crystalline ZnO Nanorods and Derived Hierarchical Nanostructures. *Langmuir*, 20, 4196-4204
7. Rezaei A., Katoueizadeh E., Zebarjad S.M. (2022). Synthesis and Characterization of ZnO Nanoparticles with Different Morphologies. *Materialstoday Chemistry*, 26, 101239
8. Santhi K., Navaneethan M., Harish S., Ponnusamy S., Muthamizhchelvan C. (2020). Synthesis and Characterization of TiO2 Nanorods by a Simple Sol-Gel Method. *Applied Surface Science* 500, 144058
9. Julian A. L., Yawei L., Soon H., Thibaut T., Daniel E. G., Asaph W. (2012). Self-Assembly of Spherical and Rod-Shaped Nanoparticles with Full Positional Control. *Advanced Materials*, 24(14),1757-1761
10. Nabiul Afrooz A.R.M., Sean T. S., Catherine J. M., Saber M. H., John J. S., Navid B. S. h. (2013). Spheres vs. rods: The shape of gold nanoparticles influences aggregation and deposition behavior. *Chemosphere,* 91(1), 93-98.
11. Isabelle P., Jean-Philippe B, Jacques P., Alain F. Surface charge, effective charge and dispersion/aggregation properties of nanoparticles, *Polymer International*, 52(4), 619-624.
12. Panikkanvalappil R. S.,Theruvakkattil S. S., Akshaya K. S, Thalappil P. (2010). Anisotropic nanomaterials: structure, growth, assembly, and functions. *Nano Reviews*, 2, 5883.
13. Raoufi D. (2013). Synthesis and microstructural properties of ZnO nanoparticles prepared by precipitation method. *Renewable Energy*, 50, 932-937.
14. Yusoff N., Ho L. N., Ong S, A., Wong Y. S., Khalik W. F. (2016). Photocatalytic activity of zinc oxide (ZnO) synthesized through different methods. *Desalination and Water Treatment*, 57(27), 12496-12507.
15. Alves T. E. P., Kolodziej C., Burda C., Franco A. (2018). Effect of particle shape and size on the morphology and optical properties of zinc oxide synthesized by the polyol mehtod. Material Design, 18, 30186-30192.
16. Masoud F. K., Zeinab F., Mohammad R. L. E., Reza S. R. (2012). Different morphologies of ZnO nanostructures via polymeric complex sol-gel method: synthesis and characterization. *Journal of Sol-Gel Science and Technology*, 64,193–199.